Diffusion Sinks in Apatite (U-Th)/He Thermochronometry: Evidence from Continuous Ramped Heating Analysis of Apatites from the KTB Deep Borehole

Hongcheng Guo[a,b*] Peter K. Zeitler[a] and Bruce D. Idleman[a]

[a] *Department of Earth and Environmental Sciences, Lehigh University, Bethlehem, PA, 18015, USA*

[b] *Department of Earth, Atmospheric, Planetary Sciences, Purdue University, West Lafayette, IN, 47907, USA*

** Correspondence to: guo750@purdue.edu*

Submitted to Earth and Planetary Science Letters

Abstract

We analyzed apatite grains from the KTB boreholes (German Continental Deep Drilling program) via the continuous ramped heating method to explore a hypothesis that some apatites contain diffusion sinks that trap ^{4}He at temperatures higher than the conventional helium closure temperature in apatite, leading to apparently over-dispersed, anomalously-old U-Th/He ages and complex laboratory diffusion behavior. The well constrained KTB samples show large intra-sample single-grain age dispersion, with most ages being older than predictions from ^{4}He radiation-damage diffusion models. Individual grains from shallower depths show a range of complex ^{4}He outgassing behaviors, including the expected low-temperature volume-diffusion loss, sudden release spikes, and a higher-temperature diffusive component. Grains from the current partial retention zone and below retain considerable helium and exhibit exclusively complex outgassing behavior. KTB samples show a systematic difference with depth in the proportion of low- and high-temperature gas-release gas components. Deeper samples, having long open-system histories, contain a greater proportion of ^{4}He that appears to be trapped compared to the simpler volume-diffusion behavior exhibited by shallower samples that experienced a simpler monotonic cooling history. The high temperature component is still present but greatly reduced in the deepest samples from the highest temperature region of the studied portion of the borehole. These observations, along with additional CRH experiments, support a model incorporating the existence of diffusion sinks in many apatites and suggest that trapping and release from these sinks is temperature sensitive. Our findings also support the suggestion that additional thermal-history information from apatites might be obtained using $^{4}He/^{3}He$ analysis, with ^{3}He providing information about trap distribution and ^{4}He providing information about the geologic thermal history.

Keywords: Apatite; (U-Th)/He; Thermochronology; Diffusion; Age Dispersion; KTB

1. Introduction

Apatite (U-Th)/He (AHe) thermochronology has become an important tool in determining the rates and timing of tectonic, surface, and other processes across varying timescales (e.g., Min et al. 2003; Reiners et al., 2005; Gautheron and Zeitler, 2020; Drake and Reiners, 2021; McDannell and Keller, 2022). Successful applications rely on an understanding of the kinetics, or more broadly speaking the systematics of helium (^{4}He) diffusion. It has been shown that in apatite, diffusion of helium has grain-specific kinetics owing to variability in factors such as grain size and radiation damage, in that the grain size defines diffusion dimension (Reiners and Farley, 2001) and radiation damage can alter diffusivity (Shuster et al., 2006; Gautheron et al., 2009; Flowers et al., 2009; Willett et al., 2017). Natural apatites should therefore show some geologically meaningful dispersion in (U-Th)/He ages. Other factors such as U-rich inclusions (Farley, 2002), parental U and Th zonation (Meesters and Dunai, 2002), grain integrity (e.g., Brown et al., 2013), uncertainties in size and shape estimation (Cooperdock et al., 2019), and ^{4}He implantation from neighborhood phases (Spiegel et al., 2009) will also complicate AHe ages and if present can make interpretation difficult by introducing additional age dispersion that is unrelated to thermal history. The international community has identified such anomalous dispersion as a critical issue (Zeitler et al., 2017a) that is receiving increased attention (Ketcham et al., 2022). A range of research approaches suggest that in addition to radiation damage, the inherent diffusivity of ^{4}He in apatite can vary between crystals due to a variety of crystal imperfections that can slow ^{4}He diffusion behavior (Gerin et al., 2017; Zeitler et al., 2017b; Fayon and Cherniak, 2021; Guo et al., 2021).

Use of continuous ramped heating (CRH, Idleman et al., 2018) provides a way to learn about grain-specific ^{4}He degassing behavior. CRH analyses have revealed to first order that the diffusion of ^{4}He in apatite does not always occur as simple volume diffusion modulated by radiation damage (McDannell, et al., 2018; Guo et al. 2021). During CRH analysis, part of the retained ^{4}He in some apatites is released at temperatures much higher than those associated with expected radiation-modulated volume diffusion, and these apatites often yield unreasonably old ages (**Fig. 1**). Zeitler et al. (2017b) and Guo et al. (2021) proposed that there could be a class of crystal imperfections in apatites that act as diffusion sinks, trapping radiogenic ^{4}He mobilized during both a sample's geologic thermal history and laboratory heating. Additionally, they proposed that apatites might record thermal histories at higher temperatures than the conventional AHe closure temperature, with the degree of trapping dependent upon the nature of their thermal histories.

In this contribution, we examine the suggestion that release of ^{4}He from diffusion sinks behaves in a systematic temperature-dependent manner. We start with reporting findings from two experiments designed to examine the temperature dependence of ^{4}He release from sinks during laboratory heating: (1) CRH analysis using different ramping rates, and (2) cycled CRH analysis. Next, we turn to geologic environments and report CRH results for an apatite suite from the German Continental Deep Drilling (KTB) borehole that records a transition from open to closed system behavior across the partial retention zone for helium in apatite. This suite should record the nature of helium closure in apatite and also provide a well characterized set of samples that have experienced different styles of thermal histories.

2 Context: Review of observations from CRH analysis of apatite

2.1 Measurement of ^{4}He degassing behavior from apatites

We used the CRH method to degas ^{4}He from apatite because it can reveal gas-release patterns during heating. Additionally, CRH is far more time-efficient than traditional step-heating because it uses fast temperature ramping during continuous heating, as opposed to the repeated heating / gettering / pumping cycle of conventional step-heating experiments. The fundamentals of the CRH method were introduced in detail by Idleman et al. (2018) and updated by Guo et al. (2021). In a CRH analysis, a single grain of apatite is heated with a continuous temperature ramp of ~30˚C/min and outgassing ^{4}He is continuously accumulated and measured. Data reduction of CRH analysis is equivalent to that of step-heating conducted using numerous steps, with the data discretized at the scale of the mass spectrometer integration time of ~10 to 20 seconds, amounting to a discretized temperature step of 5 to 10 ˚C. Higher and lower ramp rates require adjusted integration times or number of data to keep the temperature step reasonable. Measured fractional loss is corrected by first removing the system background and then subtracting the projection of the linear, time-dependent static ^{4}He blank. Beam values were not corrected for hot blank, as measurements suggest this contribution is negligible, at levels of 2×10^{-15} amps or less.

He loss by volume diffusion should result in a sigmoidal fractional ^{4}He degassing curve (*f*) and a unimodal incremental ^{4}He-degassing curve (the numerical derivative of *f* with respect to temperature, *df/dT*; hereafter we will use 'df-spectrum' for convenience) (**Fig. 1A**). Our observations from Durango apatite, known for its reproducibility of AHe ages, confirmed such unimodal gas-release behavior and consistent ^{4}He diffusion kinetics (**Fig. 1B**). For apatites in general, exactly where the peak release occurs during CRH analysis will depend on a sample's grain size, volume-diffusion kinetics, and also the CRH ramping rate. With a ramping rate of 30 ˚C/min, which is our routine analytical protocol, we typically observed peaks that represent ^{4}He

volume diffusion from the crystal lattice at ~550 to 650 ˚C (**Fig. 1C**). However, as first reported by Idleman et al. (2018) and McDannell et al. (2018), and confirmed in detail by CRH analysis of apatites from the Transantarctic Mountains (TAM; Guo et al., 2021), some grains also show complex gas release that significantly departs from predictions that assume only volume diffusion. These complex patterns include gas released as sharp spikes that occur within one data-acquisition block, and most notably, a secondary ^{4}He component released at higher temperatures, very often in the form of a discrete peaks at between ~800 to 900˚C (**Fig. 1D**).

2.2 Is gas-release from the diffusion sinks temperature-dependent?

In the model proposed by Guo et al. (2021), the higher temperature release seen in complex CRH analyses as well as any sharp spikes are the consequence of trapping of ^{4}He into sinks. This trapping occurs during a sample's geologic thermal history as well as when it is heated for laboratory analysis. This stems from the extended random walk taken by ^{4}He atoms during the diffusion process – such walks are sufficiently long (up to meters) with high numbers of jumps such that even a small volume of sinks present in a crystal will still result in a high probability of an atom encountering a sink. Clearly the laboratory data show that escape from such sinks occurs at high temperatures, but a key question for understanding diffusion systematics and apatite thermochronological data is the degree to which this component shows a kinetic as opposed to a threshold response.

To test this, we first conducted CRH analysis on apatite grains using widely different ramp rates of 1.5 ˚C/min, 6 ˚C/min, and 90 ˚C/min. Volume-diffusion theory predicts that peak gas release will occur at higher temperatures at higher CRH ramp rates and vice versa (see simulations by Idleman et al. (2018)), and this is also what we observed in both Durango apatites and a

subgroup of the TAM apatites that have unimodal gas-release curves (**Fig. 2A**). For those TAM apatites that also show high-temperature release components, we find that both the low- and high-temperature release peaks shift in location as a systematic function of ramp rate (**Fig. 2B**).

We then conducted cycled CRH experiments using three successive CRH sessions for single-grain samples. Each CRH session started at ~200 ˚C with a ramping rate of 30 ˚C/min, and gases were pumped away between the sessions. The first session was stopped at ~470 ˚C, a point where significant volume-diffusion-related gas often starts to accumulate; the second session was stopped at ~700 ˚C where substantial high-temperature gas release often starts; and the last session was the same as a standard CRH analysis extending from 200˚C to total degassing of a sample by about ~1000 ˚C. We found that a Durango apatite has most of its ^{4}He released across the first two heating sessions with the total degassing happening no later than ~800 ˚C (**Fig. 2C**). The Arrhenius relations established from the three heating sessions are close to identical (**Fig. 2D)**. For a TAM apatite that shows complex ^{4}He release, after the first two CRH sessions during which a considerable amount of ^{4}He has been released, the last CRH session presents little gas-release until ~600 ˚C, above which the incremental ^{4}He release of the last heating session itself has a unimodal shape. The linear part of the Arrhenius data from the first and the third heating sessions document significantly different apparent retentivity with the second session seeming to document a transition. Gas release from the third session is quite systematic and indicative of volume-diffusion behavior.

3. Study material: The KTB apatites

Apatites from the KTB drill holes are excellent material with which to examine a ^{4}He diffusion model that includes sinks. Partly this is because they offer a chance to look at helium retention

and closure across the partial retention zone, and partly this is because samples from varying depths experienced very different thermal histories: for an extended time, samples at greater depths have been close to isothermal at temperatures near helium closure, in contrast to shallow samples that initially cooled monotonically and since then have been a closed system. The apatites we used were obtained from the KTB pilot hole with depths extending from a few hundred meters to nearly 4000 meters, and also from the KTB main hole that extends deeper (Wagner et al., 1997). Much of the studies of the KTB's thermal history (e.g., Wagner et al., 1997; Wolfe and Stockli, 2010) have been centered on the KTB main hole, but as the pilot hole is only ~200 meters from the pilot hole, we assume similar thermal histories were shared by the two locations.

For depths from the surface to 4 km, Wagner et al. (1997) proposed that the uppermost 1.8-km block of the hole experienced a cooling rate of ~2˚C/My from the late Cretaceous to ~25 Ma followed by little erosion, and that the underlying 1.8-4.3-km block had a cooling rate of ~ 2.9 ˚C/My from the late Cretaceous to ~ 50 Ma, again followed by little erosion. Wolfe and Stockli et al. (2010) reported a slightly revised version, which we used in the discussion of our results. Similar thermal histories were also inferred by Coyle et al. (1997) for the slow cooling interval from the late Cretaceous to the middle Cenozoic, except that they proposed minor reheating at ~ 1.5 ˚C/My from the Oligocene to the present. What is most relevant to our study is that, to first order, the samples we analyzed, from near-surface to ~4000 meters, represent broadly three types of thermal histories (**Fig. 3C**): apatites that have been in a closed system for a long period of time, apatites that are now within a conventionally defined helium partial retention zone (PRZ; ~40 – 80 ˚C; Stockli et al., 2000), and apatites that have been and still are open systems today.

4. Analytical methods for KTB samples

We examined 11 KTB samples from depths ranging from 316 m to 4348 m, and for each sample, we analyzed 3 – 9 grains depending on grain availability. Note that the naming scheme of the samples (**Fig. 4**) reflects their depth. Ten of the samples, from the pilot drill hole, are the same separates as those reported on by Warnock et al. (1997). We separated apatites from a deeper sample from rock taken from the adjacent main drill hole. Each apatite grain was measured by CRH with a 30 ˚C/min ramping rate at the Lehigh University noble-gas geochronology lab using detailed procedures reported by Guo et al. (2021). New to this study because some signals from deeper samples were very low, we documented typical uncertainties in the ^{4}He beam current to be better able to distinguish signal from noise in displaying CRH data (i.e., raw *df* plots in Supplementary Material **Fig**. **A1**). Parental U-Th-Sm isotopes were measured by dissolution and isotope dilution at the Arizona Radiogenic Laboratory with the method reported by Reiners and Nicolescu (2006). For each apatite grain, we obtained its ^{4}He *df* spectrum and single-grain helium age. We also used the thermal histories determined by Wolfe and Stockli (2010) and our measured eU and grain size (reported in the Data repository; see section **Data Availability**) to predict AHe ages using the RDAAM model (Flowers et al., 2009), allowing us to explore the degree to which ^{4}He retention could be explained just by grain size and radiation damage.

5. KTB results

5.1. Apatite (U-Th)/He ages

As would be expected, our youngest single-grain AHe ages become younger with depth, nearing zero age for the deepest samples (**Fig. 3A, B**). Most of our geometric mean ages for all grains at a particular depth are close to age measurements made by Warnock et al. (1997) (**Fig. 3B,** triangles) who at that time were only able to analyze milligram-sized aliquots of apatite grains –

their ages would approximate an integration across our single-grain ages. At all depths our KTB results show significant age dispersion, and measurable ^{4}He was present at all depths including those currently having temperatures of >100˚C, conditions under which conventional understanding would predict ages to be zero (see RDAAM modeling in section 5.3). A number of grains in several samples well exceed measured apatite fission-track ages (**Fig. 3B**), an inverted relationship that has been widely observed (e.g., Fitzgerald et al., 2006; Ault et al., 2019; Guo et al., 2021).

5.2. CRH ^{4}He outgassing behavior

The *df* spectra for these apatite grains are summarized in **Fig. 4**. For clarity when multi-grain analyses are overlaid, these data are presented using an 11-point median filter, so any gas spikes are removed while the overall shapes of the spectra are retained and more clearly illustrated. Supplementary **Fig**. **A1** shows unfiltered *df* spectra for each individual grain.

The *df* spectra from the KTB samples fall into three categories.

(1) The single grains from the shallowest three samples, KTB-316, KTB-435, and KTB-920, with depths no greater than 1 km and present-day temperatures lower than 40˚C, show both simple and complex *df* spectra (**Fig. 4**, blue lines). For those apatites that have complex *df* spectra, most of the ^{4}He is released during lower laboratory-heating temperatures that peaked at ~500-600 ˚C, with only one exception.

(2) Samples at depths equivalent to temperatures within the PRZ for helium in apatite (~40 – 80˚C; ~1.25 to 2.75 km) show only complex *df* spectra in which a substantial amount of ^{4}He is released at both low and high temperatures (KTB-1901 and KTB-2353; **Fig. 4**, green lines). The

high-temperature gas components occur as either a discrete peak or a broader shoulder, often with the presence of significant gas spikes as well.

(3) In samples at depths equivalent to temperatures above the PRZ, the total ^{4}He content of these deeper apatite grains is much lower, but almost all of this ^{4}He is released at high laboratory heating temperatures (KTB-2954 and deeper; **Fig. 4**, red lines). In many but not all samples, this higher-temperature release manifests as a discrete peak but this release occurs over a range of temperatures.

5.3. Expected age variation due to varying radiation damage and grain size

Volume diffusion in apatites is known to be controlled to second order by radiation damage and grain size. Because we are interested in how other factors like trapping might contribute to age dispersion, we first need to evaluate how much damage and size might be responsible for the observed variability in ages (**Fig. 3**). This is particularly important for the KTB suite because some of the deeper samples have been residing in the PRZ for an extended time, which will accentuate even small differences in diffusivity.

Our KTB apatite suite has a broad range of effective uranium (eU) (mostly from ~15 to 80 ppm) and in F_T spherical-equivalent radii (ranging from ~40 to 80 μm), again with just a few exceptions. For any one sample whose grains shared an exact thermal history, both higher eU and radius should lead to greater retentivity and so older ages, but we did not find a positive correlation between age and eU, nor between age and grain size. There is a moderate positive correlation between age and grain size for the grains from the shallowest three samples that are in a closed system at present-day.

To further assess how variation in grain size and radiation damage might explain dispersion, we performed forward modeling using the HeFTy code (Ketcham, 2005) using the KTB thermal histories proposed by Wolfe and Stockli (2010), and our measured eU and grain radii as inputs. These predicted ages show only moderate dispersion for the apatites from the shallow and PRZ-location segments of the KTB boreholes (**Fig. 3A, B**), and quickly converge to near-zero ages for samples deeper than ~ 3km.

6. Discussion

We first review an update to the ^{4}He transport model proposed by Guo et al. (2021). We next discuss the results from CRH experiments with different ramping rates and cycled heating that suggest the release for ^{4}He from sinks is temperature sensitive. Finally, after setting out predictions for what we expected to see in the KTB suite, we discuss the implications of our CRH observations.

6.1. ^{4}He diffusion in the presence of sinks

We hypothesize that there are three different states of helium diffusion systematics in apatite. (1) In 'perfect' apatites having a pristine lattice, ^{4}He transport occurs by simple volume diffusion at the maximum observed rate determined by an activation energy E_a and diffusion coefficient D_o that derive from fundamental properties of the lattice (Djimbi et al. 2015). For such hypothetical samples, single-grain AHe ages should be consistent within analytical error and the CRH degassing behavior should be highly reproducible with a single outgassing peak that corresponds closely to that predicted by their diffusion parameters. (2) Perfect apatite will of course never exist – even just the substitution of U and Th in the lattice will deform it. More generally, natural apatites will inevitably have various kinds of fine-scale lattice defects (due, for example to

factors like radiation damage, deformation, or grain chemistry), but such helium in such grains will still broadly exhibit volume diffusion behavior. The diffusivities of such samples will vary and show some extent of geologically and geochemically meaningful dispersion in AHe ages. CRH *df* spectra from these apatites would still be unimodal but show some variation in shape, width, and location of the single, lower-temperature, gas-release peaks. Many dated apatites that produce relatively well-reproduced ages would fall into this category. However, the variations in diffusivity that can occur are not limited to radiation damage defects, and as observed by Guo et al. (2021), there is good reason to believe that each apatite grain will have a unique diffusivity determined by its defect profile. (3) The third phenomenon that would control diffusion in natural apatites is the presence of sinks that can trap radiogenic ^{4}He as it is transported by volume diffusion. Such imperfections would take the form of voids larger than fine-scale lattice defects, e.g., fluid inclusions, and are likely present in many mineral grains (Watson and Cherniak, 2003; Zeitler et al., 2017b). The presence of a trapped component would explain both the high-temperature release seen during some CRH analyses as well as sharp release spikes, which could be associated with occasional voids located very close to the grain surface. Samples of apatite grains containing such sinks would exhibit anomalously old ages and higher age dispersion.

6.1.1. Nature and dynamics of trapping into sinks

How ^{4}He comes to be trapped in to sinks will depend on the atom-scale nature of diffusion involving a random walk based on jumps between sites. As discussed by Djimbi et al. (2015) and Zeitler et al. (2017b), escape from a grain will involve meters of travel and 10^9 or more jumps, and this means that it is very likely that diffusing ^{4}He atoms will encounter even a very small total volume of sinks in the form of pores or voids. Because the solubility of helium in apatite is

very low (Zeitler et al., 2017b), atoms entering into larger sinks will not easily return to the lattice. The source of trapped components in apatite need not be "excess" in the sense of being externally derived, but just be radiogenic helium derived from the grain itself. This component would be excess only with respect to conventional expectations about closure to diffusion in simple grains.

This model (**Fig. 5**) for trapping has implications for CRH *df* spectra. First, because apatites undergoing CRH analysis experience two episodes of diffusion (geologic thermal history and then heating in the lab), trapping will occur both in nature and in the lab. This means that the component of ^{4}He released at temperatures above those predicted by simple volume diffusion will include contributions from both lattice-hosted and geologically trapped ^{4}He, so the relative sizes of the two release peaks is not a simple measure of "good" expected components versus a "bad" trapped components. Second, for a given volume of sinks, the degree of geologic trapping will depend on the sample's thermal history because trapping will occur in proportion to the time the sample spends at temperatures at which radiogenic helium is mobile (Zeitler et al., 2021). For example, a sample cooled very rapidly will accumulate all its helium at low temperatures and little or none will be trapped because there is little or no diffusion taking place. At the other extreme, a sample stagnated at temperatures within the partial retention zone might trap large amounts of radiogenic helium that classical theory would assume to have diffused readily and been lost. We discuss the thermochronological implications of this below.

6.2. Temperature-sensitive ^{4}He-release from diffusion sinks

If there is a chance that helium trapped in sink-bearing grains has the potential to yield additional thermal-history information (Zeitler et al., 2021), several important questions follow about the

mechanism of trapping and release and whether this is a systematic phenomenon with a kinetic response. Does trapping happen at even very high metamorphic conditions, well above PRZ temperatures? Is the release from sinks kinetically controlled, or a threshold process?

In our CRH experiments using different ramping rates, not only does the lower-temperature release shift with temperature as expected from volume-diffusion theory but a shift is also seen in the high-temperature release (i.e., peak release shifts to higher temperatures when the ramping rates are higher, and vice versa) (**Fig. 2A, B**). The shift in higher-temperature release with ramping rate (laboratory thermal history) is strong evidence against a threshold-controlled mechanism and favors kinetic control as the mechanism. The observation that in some cases the high-temperature release is spread across a wider range could be evidence for range of different sink types.

In our cycled heating experiments, the Durango apatite has most of its ^{4}He released in the first two of the three heating sessions (**Fig. 2A**), and three sessions define almost same kinetics in the Arrhenius plot (**Fig. 2D**). The Durango results show no evidence that heating to high temperatures significantly modifies the diffusion kinetics. In contrast, the TAM apatite shows a significant amount of gas released in the third heating session, significantly offsetting from the early Arrhenius trend, which is consistent with the higher-temperature release of sink-hosted ^{4}He (**Fig. 2E**). In its Arrhenius plot (**Fig. 2F**), we interpret the linear part of data from the first heating session as the kinetics of volume diffusion in the crystal lattice; in the second heating session, the Arrhenius data map the same trend with but progressively roll over towards more a retentive regime defined by ^{4}He-release from sinks. Finally, the last heating session defines another linear part of Arrhenius data dominated by the release of sink-hosted ^{4}He. This

systematic high-temperature trend is interesting in that it might reflect the combined effects of two temperature-dependent processes: escape from sinks, and then normal volume diffusion through the lattice.

Overall, these experiments suggest that ^{4}He-release from diffusion sinks is temperature dependent.

6.3. Implications of KTB results

6.3.1. Measured AHe ages versus RDAAM predictions

At all depths within the KTB boreholes our measured single-grain ages are older than ages predicted using the RDAAM model given the inferred thermal histories, grain sizes, and eU values of the analyzed samples (**Fig. 3A**). Some individual grains showing simple unimodal ^{4}He outgassing behavior fall close to the RDAAM predictions, but in general observed ages are far older, and clearly cannot be explained by size and radiation-damage effects. Older grains are more likely to have complex *df* spectra, but not in every case. Older ages from samples showing unimodal spectra likely reflect variations in diffusion kinetics beyond those accounted for by the RDAAM model as suggested by Guo et al. (2021): the kinetic variability of ^{4}He diffusion is generally wider than what grain size and radiation damage suggest, probably due to the presence of varying amounts and types of fine-scale lattice imperfections. The overlap between our youngest single-grain ages and the RDAAM predictions suggests that the RDAAM model predictions provide a lower boundary for dispersed groups of ages, and thus supports the empirical observation that in a dispersed AHe dataset measured from surface samples, the youngest single-grain ages often give meaningful apparent ages consistent with geological

constraints and expectations from the RDAAM model (e.g., Fitzgerald et al., 2006, Guo et al. 2021, He et al., 2021).

6.3.2. ^{4}He *df* spectra and diffusion systematics at different depths

Because our samples from the KTB borehole span the entire AHe PRZ, these samples do not share a set of common thermal histories, although their thermal histories are linked. The shallowest samples cooled monotonically through the PRZ at slow rates of ~1˚C/m.y. and have remained cool and closed to diffusion since then, whereas the deepest samples we examined have been warm for tens of millions of years and never in fact ascended into the conventional PRZ (**Fig. 3C**). This provides an opportunity to view the closure process and also to examine ^{4}He trapping under different thermal histories.

Our measured KTB df spectra (**Fig. 4**) are quite consistent with predictions from our conceptual model for diffusion systematics in apatite (Section 6.1, above). Shallow samples that have been closed systems for tens of m.y. have *df* spectra dominated by low-temperature release peaks, with only minor secondary peaks that reflect small amounts of trapping during faster transit of the PRZ as well as additional trapping during lab heating. Samples currently close to or within the PRZ show intermediate behavior, with a greater fraction of their helium budget being trapped in sinks and released at higher laboratory temperatures. Finally, the deepest samples, which should have no conventional radiogenic He, release their helium only at high temperatures in the laboratory. In short, the *df* spectra we observed across the KTB suite show that different thermal histories will lead to different release spectra. As a function of depth and thus thermal history, this systematic shift in internal ^{4}He distribution between lattice- and sink-hosted components is clearly shown by comparing the ratio of low-temperature and high-temperature release (**Fig. 6**).

6.3.3. Inferences from deeper samples about sink kinetics

The observed variation in helium content with depth has important implications for the behavior of sinks. *df* spectra clearly show that the helium present in our deeper samples is confined to sinks. Presumably this reflects the continuous production of radiogenic ^{4}He and its volume-diffusion mobility at high temperatures: the only helium that is retained is helium that has been trapped. But the total helium content in our samples drops with depth, and by ~4.4 km and ~130 ˚C, the trapped helium content is near zero. This suggests that over timescales of tens of m.y. at temperatures of >~120˚C, the sinks in these KTB grains were open to helium loss.

This extended residence in the PRZ compares well to the temperatures of some ~800˚C required to outgas sinks over a few minutes in the laboratory. Lab outgassing at 800˚C over an averaged timescale of some 5 minutes corresponds to a Dt/a^2 of ~0.14, assuming an activation energy of 33 kcal/mol and D_o of 0.25 cm^2/s. Using the same parameters, the heating duration at 120˚C to obtain the same Dt/a^2 would be about 40 m.y.. The crude episodic-loss calculations suggest that This observed scaling in time and temperature supports a kinetic mechanism for release out of sinks that applies to both natural settings and laboratory release.

6.4. Summary and considerations for future research

Much exploration and practice of the (U-Th)/He method has been based on describing the diffusion of ^{4}He using models that assume uniform volume diffusion that is somewhat modified by radiation damage accumulation and annealing models. All of those models fail to explain much of the widely observed over-dispersion of AHe ages. We suggest that a model that incorporates trapping into sinks as well as variations in apatite diffusivity will do a better job

describing these observations. Development of a quantitative model will require several new lines of research.

First, because of the likelihood that each apatite crystal represents a single thermochronometer whose diffusion parameters are likely to vary more than is considered by current models, dispersed ages are likely to be geologically meaningful in many cases. However, much more effort will be needed to characterize the range of possible kinetic variations for helium diffusion in apatite, and a means of determining the kinetics of each analyzed grain will be needed. $^{4}He/^{3}He$ analysis (Shuster and Farley, 2005), in which the ^{3}He release in the laboratory can be used to determine kinetics, is an obvious way forward.

Second, more experimental and theoretical material-science work will be needed to better understand what sort of features can act as sinks for diffusing helium in apatite and over what range of conditions they operate. Do sinks change their properties (e.g., annealing at high temperatures, Recanati et al., 2017) during a sample's geologic evolution or during laboratory analysis? Can deformation cause such features to develop, possibly during closure at lower temperatures (Fayon and Cherniak, 2021)? Is helium trapping into sinks seen in other minerals besides apatite?

Finally, given the kinetic response we have documented for helium release from sinks, the possibility arises that a hybrid $^{4}He/^{3}He$ CRH approach might extract more thermal-history information from single grains, with trapping in this case being a positive phenomenon rather than a nuisance (Zeitler et al., 2021). In $^{4}He/^{3}He$ analysis, proton-induced ^{3}He is created artificially with a uniform distribution throughout apatite grains after the sample has experienced

its geologic history. Therefore, ^{3}He measurements made in the laboratory should faithfully reflect the trapping dynamics of any sinks present. In contrast, the distribution of ^{4}He in lattice sites and sinks would be a function of both the sample's geologic thermal history and the trapping dynamics of sinks. With the trapping information gleaned from the ^{3}He release, it should be possible to invert *df* spectra for thermal history, somewhat analogous to the multi-diffusion domain (MDD) approach for K-felspar ^{40}Ar/^{39}Ar analysis, where ^{39}Ar release in the lab determines the kinetics of the samples and also the diffusion-domain distribution, and the ^{40}Ar/^{39}Ar reflects that plus the influence of the sample's geological thermal history (Harrison and Lovera, 2014).

7. Conclusion

Our single-grain analysis of apatites from the KTB boreholes reveals single-grain ages that are greater than zero even at depth of ~4 km. For apatites that exhibit complex *df* spectra from CRH analysis, we find a depth-dependent proportion of ^{4}He released at low temperatures versus at high temperatures. Those findings together with CRH laboratory experiments provide additional evidence that there are diffusion sinks in many apatites that can reversibly trap ^{4}He. The data also show that ^{4}He release from such sinks is temperature dependent, opening up the possibility of extracting more thermal history information from apatites.

CRediT authorship contribution statement

HG: Conceptualization, Methodology, Formal analysis, Investigation, Data Curation, Writing – Original Draft, Writing – Review & Editing, Visualization. PKZ, BDI: Conceptualization, Funding acquisition, Methodology, Resources, Writing – Review & Editing.

Acknowledgments

Both this work and part of HG's graduate study were supported by the National Science Foundation [grant EAR-1726350 to PKZ and BDI]; We thank the Department of Earth and Environmental Sciences, Lehigh University for a graduate student research fund to HG that in part supported the laboratory analysis. We thank Uttam Chowdhury and Peter Reiners at the Arizona Radiogenic Dating Laboratory for Uranium-Thorium-Samarium measurements.

Data Availability

Research Data associated with this article can be accessed via Harvard Dataverse at https://doi.org/10.7910/DVN/MMTRV2.

References

Ault A. K., Gautheron C. and King G. E. (2019) Innovations in (U–Th)/He, fission track, and trapped charge thermochronometry with applications to earthquakes, weathering, surface-mantle connections, and the growth and decay of mountains. *Tectonics* **38,** 3705-3739.

Brown, R. W., Beucher, R., Roper, S., Persano, C., Stuart, F., & Fitzgerald, P. (2013) Natural age dispersion arising from the analysis of broken crystals. Part I: Theoretical basis and implications for the apatite (U–Th)/He thermochronometer. *Geochimica et Cosmochimica Acta **122***, 478-497.

Cooperdock E. H., Ketcham R. A. and Stockli D. F. (2019) Resolving the effects of 2-D versus 3-D grain measurements on apatite (U–Th)/He age data and reproducibility. *Geochronology* **1,** 17-41.

Coyle D. A., Wagner G. A., Hejl E., Brown R. and den Haute P. V. (1997) The Cretaceous and younger thermal history of the KTB site (Germany): apatite fission-track data from the Vorbohrung. *Geol. Rundsch.* **86,** 203-209.

Djimbi D. M., Gautheron C., Roques J., Tassan-Got L., Gerin C. and Simoni E. (2015) Impact of apatite chemical composition on (U-Th)/He thermochronometry: An atomistic point of view. *Geochim. Cosmochim. Acta* **167,** 162-176.

Drake H. and Reiners P. W. (2021) Thermochronologic perspectives on the deep-time evolution of the deep biosphere. *Proceedings of the National Academy of Sciences* **118,** e2109609118.

Farley, K. A. (2002) (U-Th)/He dating: Techniques, calibrations, and applications. *Reviews in Mineralogy and Geochemistry* **47(1)**, 819-844.

Fayon A. K. and Cherniak D. J. (2021) Helium diffusion in experimentally deformed Durango apatite single crystals. *17th International Conference on Thermochronology.*

Fitzgerald P. G., Baldwin S. L., Webb L. E. and O'Sullivan P.,B. (2006) Interpretation of (U–Th)/He single grain ages from slowly cooled crustal terranes: a case study from the Transantarctic Mountains of southern Victoria Land. *Chem. Geol.* **225,** 91-120.

Flowers R. M., Ketcham R. A., Shuster D. L. and Farley K. A. (2009) Apatite (U–Th)/He thermochronometry using a radiation damage accumulation and annealing model. *Geochim. Cosmochim. Acta* **73,** 2347-2365.

Gautheron C., Tassan-Got L., Barbarand J. and Pagel M. (2009) Effect of alpha-damage annealing on apatite (U-Th)/He thermochronology. *Chem. Geol.* **266,** 157-170.

Gautheron C. and Zeitler P. K. (2020) Noble gases deliver cool dates from hot rocks. *Elements: An International Magazine of Mineralogy, Geochemistry, and Petrology* **16,** 303-309.

Gerin C., Gautheron C., Oliviero E., Bachelet C., Djimbi D. M., Seydoux-Guillaume A., Tassan-Got L., Sarda P., Roques J. and Garrido F. (2017) Influence of vacancy damage on He diffusion in apatite, investigated at atomic to mineralogical scales. *Geochim. Cosmochim. Acta* **197,** 87-103.

Guo H., Zeitler P. K., Idleman B. D., Fayon A. K., Fitzgerald P. G. and McDannell K. T. (2021) Helium diffusion systematics inferred from continuous ramped heating analysis of Transantarctic Mountains apatites showing age overdispersion. *Geochim. Cosmochim. Acta* **310,** 113-130.

Harrison T. M. and Lovera O. M. (2014) The multi-diffusion domain model: past, present and future. *Geological Society, London, Special Publications* **378,** 91-106.

He J., Thomson S. N., Reiners P. W., Hemming S. R. and Licht K. J. (2021) Rapid erosion of the central Transantarctic Mountains at the Eocene-Oligocene transition: Evidence from skewed (U-Th)/He date distributions near Beardmore Glacier. *Earth Planet. Sci. Lett.* **567,** 117009.

Idleman B. D., Zeitler P. K. and McDannell K. T. (2018) Characterization of helium release from apatite by continuous ramped heating. *Chem. Geol.* **476,** 223-232.

Ketcham R. A. (2005) Forward and inverse modeling of low-temperature thermochronometry data. *Reviews in mineralogy and geochemistry* **58,** 275-314.

Ketcham R. A., Tremblay M., Abbey A., Baughman J., Cooperdock E., Jepson G., Murray K., Odlum M., Stanley J. and Thurston O. (2022) Report from the 17th International Conference on Thermochronology. DOI: 10.1002/essoar.10511082.1

McDannell K. T., Zeitler P. K., Janes D. G., Idleman B. D. and Fayon A. K. (2018) Screening apatites for (U-Th)/He thermochronometry via continuous ramped heating: He age components and implications for age dispersion. *Geochim. Cosmochim. Acta* **223,** 90-106.

McDannell K. T. and Keller C. B. (2022) Cryogenian glacial erosion of the central Canadian Shield: The “late” Great Unconformity on thin ice. *Geology*

Meesters A. and Dunai T. J. (2002) Solving the production–diffusion equation for finite diffusion domains of various shapes: Part II. Application to cases with α-ejection and nonhomogeneous distribution of the source. *Chem. Geol.* **186,** 57-73.

Min K., Farley K. A., Renne P. R. and Marti K. (2003) Single grain (U–Th)/He ages from phosphates in Acapulco meteorite and implications for thermal history. *Earth Planet. Sci. Lett.* **209,** 323-336.

Recanati A., Gautheron C., Barbarand J., Missenard Y., Pinna-Jamme R., Tassan-Got L., Carter A., Douville É, Bordier L. and Pagel M. (2017) Helium trapping in apatite damage: Insights from (U-Th-Sm)/He dating of different granitoid lithologies. *Chem. Geol.* **470**, 116-131.

Reiners P. W., Ehlers T. A. and Zeitler P. K. (2005) Past, present, and future of thermochronology. *Reviews in Mineralogy and Geochemistry* **58,** 1-18.

Reiners P. W. and Farley K. A. (2001) Influence of crystal size on apatite (U–Th)/He thermochronology: an example from the Bighorn Mountains, Wyoming. *Earth Planet. Sci. Lett.* **188,** 413-420.

Reiners, P. W., and Nicolescu, S. (2006) Measurement of parent nuclides for (U-Th)/He chronometry by solution sector ICP-MS. *ARHDL Report* **1**, 1-33.

Shuster D. L., Flowers R. M. and Farley K. A. (2006) The influence of natural radiation damage on helium diffusion kinetics in apatite. *Earth Planet. Sci. Lett.* **249,** 148-161.

Shuster D. L. and Farley K. A. (2005) 4He/3He thermochronometry: Theory, practice, and potential complications. *Reviews in Mineralogy and Geochemistry* **58,** 181-203.

Spiegel C., Kohn B., Belton D., Berner Z. and Gleadow A. (2009) Apatite (U–Th–Sm)/He thermochronology of rapidly cooled samples: the effect of He implantation. *Earth Planet. Sci. Lett.* **285,** 105-114.

Stockli D. F., Farley K. A. and Dumitru T. A. (2000) Calibration of the apatite (U-Th)/He thermochronometer on an exhumed fault block, White Mountains, California. *Geology* **28,** 983-986.

Wagner G. A., Coyle D. A., Duyster J., Henjes-Kunst F., Peterek A., Schröder B., Stöckhert B., Wemmer K., Zulauf G. and Ahrendt H. (1997) Post-Variscan thermal and tectonic evolution of the KTB site and its surroundings. *Journal of Geophysical Research: Solid Earth* **102,** 18221-18232.

Warnock A. C., Zeitler P. K., Wolf R. A. and Bergman S. C. (1997) An evaluation of low-temperature apatite U-Th/He thermochronometry. *Geochim. Cosmochim. Acta* **61,** 5371-5377.

Watson E. B. and Cherniak D. J. (2003) Lattice diffusion of Ar in quartz, with constraints on Ar solubility and evidence of nanopores. Geochimica et Cosmochimica Acta 67, 2043-2062.

Willett C. D., Fox M. and Shuster D. L. (2017) A helium-based model for the effects of radiation damage annealing on helium diffusion kinetics in apatite. *Earth Planet. Sci. Lett.* **477,** 195-204.

Wolfe M. R. and Stockli D. F. (2010) Zircon (U–Th)/He thermochronometry in the KTB drill hole, Germany, and its implications for bulk He diffusion kinetics in zircon. *Earth Planet. Sci. Lett.* **295,** 69-82.

Zeitler, P.K., Brown, R., Hackspacher, P. (2017a) Better tools for tracing the thermal history of rocks (Meeting report: Thermo2016: The 15th International Conference on Thermochronology; Maresias, Brazil, 18-23 September 2016). EOS, 98, DOI: 10.1029/2017EO073479.

Zeitler P. K., Enkelmann E., Thomas J. B., Watson E. B., Ancuta L. D. and Idleman B. D. (2017b) Solubility and trapping of helium in apatite. *Geochim. Cosmochim. Acta* **209,** 1-8.

Zeitler P., Guo H., Idleman B. and McDannell K. (2021) He Diffusion Systematics in Apatite. *ESS Open Archive.* September 09, 2021. DOI: 10.1002/essoar.10507948.1.

Figure Captions

Figure 1. Incremental ^{4}He release curves (*df* spectra). (A) Theoretical volume diffusion behavior of apatite using diffusion coefficient (D_o) of 50 cm^2/s and activation energy (E_a) of 33 kcal/mol. Three simulations were performed on grains with spherical geometries of 70, 80, and 100 μm, illustrated by three curves from left to right, highlighted by subtle differences in peak gas-release temperature. (B) Observed example *df* spectra of Durango apatites. Panels (C) and (D) show observations from TAM (Transantarctic Mountain) apatite. Data for (A) are reported in the Data repository. Data for (B), (C), and (D) are adapted from Guo et al. (2021).

Figure 2. Result from CRH experiments with different ramping rates and multi-session CRH experiments. (A), (B) Varying temperature at which peak gas-releases occur from CRH analysis using different ramping rates. The peaks that reflect volume diffusion (i.e., the sole peak for simple *df* spectra and the first peak for complex *df* spectra) happen at higher temperatures with a faster heating session, and vice versa for both Durango Apatites (A) and TAM apatites (B). For the TAM apatites that have complex df spectra, the secondary gas peaks also shift toward the right with faster CRH. For clarity and readability, the plotted data are 11-point median-filtered. Data are available in the Data Repository. (C), (D) *df* spectra and Arrhenius plots for a single-grain Durango apatite that undergoes three sessions of CRH. (E), (F) *df* spectra and Arrhenius plots for a single-grain TAM apatite, which would have a complex df spectrum with a typical single-pass CRH experiment, that undergoes three sessions of CRH.

Figure 3. Ages of KTB apatites. (A) (B) Measured single-grain AHe ages and mean ages for grains plotted versus depth and present-day temperature; also presented are measured AHe and AFT ages from Warnock et al. (1997) and predicted single-grain AHe ages using the RDAAM model. Uncertainties are 2-sigma. The single-grain AHe ages in (A) that come from apatites exhibiting simple *df* spectra are the circles marked by heavier boundaries. (C) Thermal histories of the analyzed KTB samples, after Wolfe and Stockli (2010).

Figure 4. Incremental ^{4}He release curves (*df* spectra) for KTB apatites. The upper left plot is a summary of the results from all samples. The rest of the plots showcase single-grain analyses for individual samples sourced from various depths. Each line represents a median-filtered result of the single-grain analysis. Blue: samples with closed-system behavior; green (< ~3 km) and red (> ~3 km) are samples in open systems. The shaded error band reported 2-sigma uncertainty envelops of the measured *df* due to the beam uncertainty. Guo et al. (2021) found that the 1-sigma uncertainty of measured temperatures is ~8 ˚C using a size-adjusted inter-grain comparison of spherical Durango apatite crystals. Readers are referred to Fig. A1 in the Supplementary Material for individual *df* plots for each grain. Data are reported in Data repository.

Figure 5. Conceptual illustration of ^{4}He accumulation rate in geological time (B) and the corresponding incremental ^{4}He release (*df*) in lab observation (C) for three samples that have various thermal histories.

Figure 6. Comparison of low-temperature and high-temperature gas components. 700˚C is used as a rough divide between low- and high-temperature components. (B) presents the same content as in (A) but highlights the mean values.

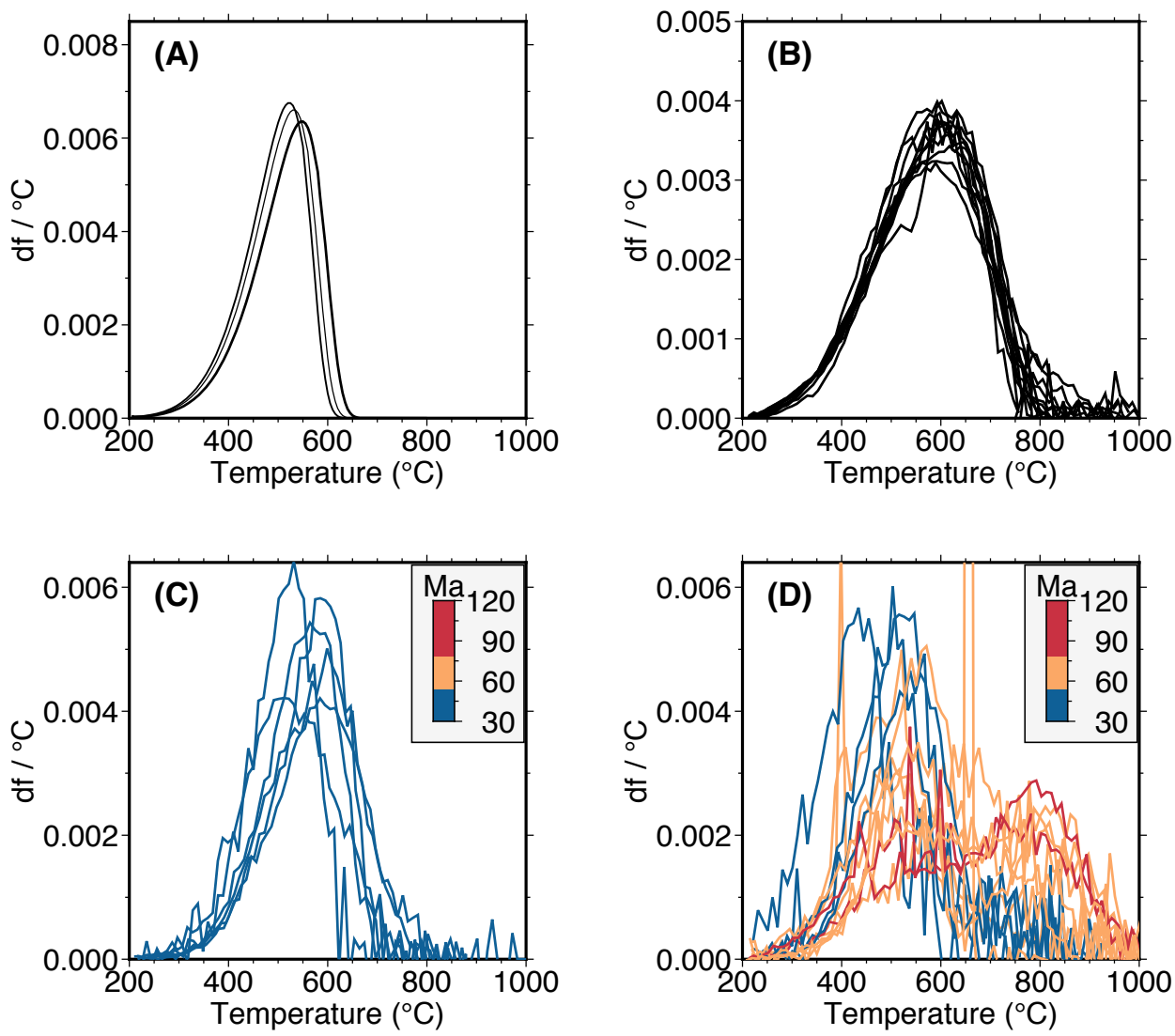

Fig. 1

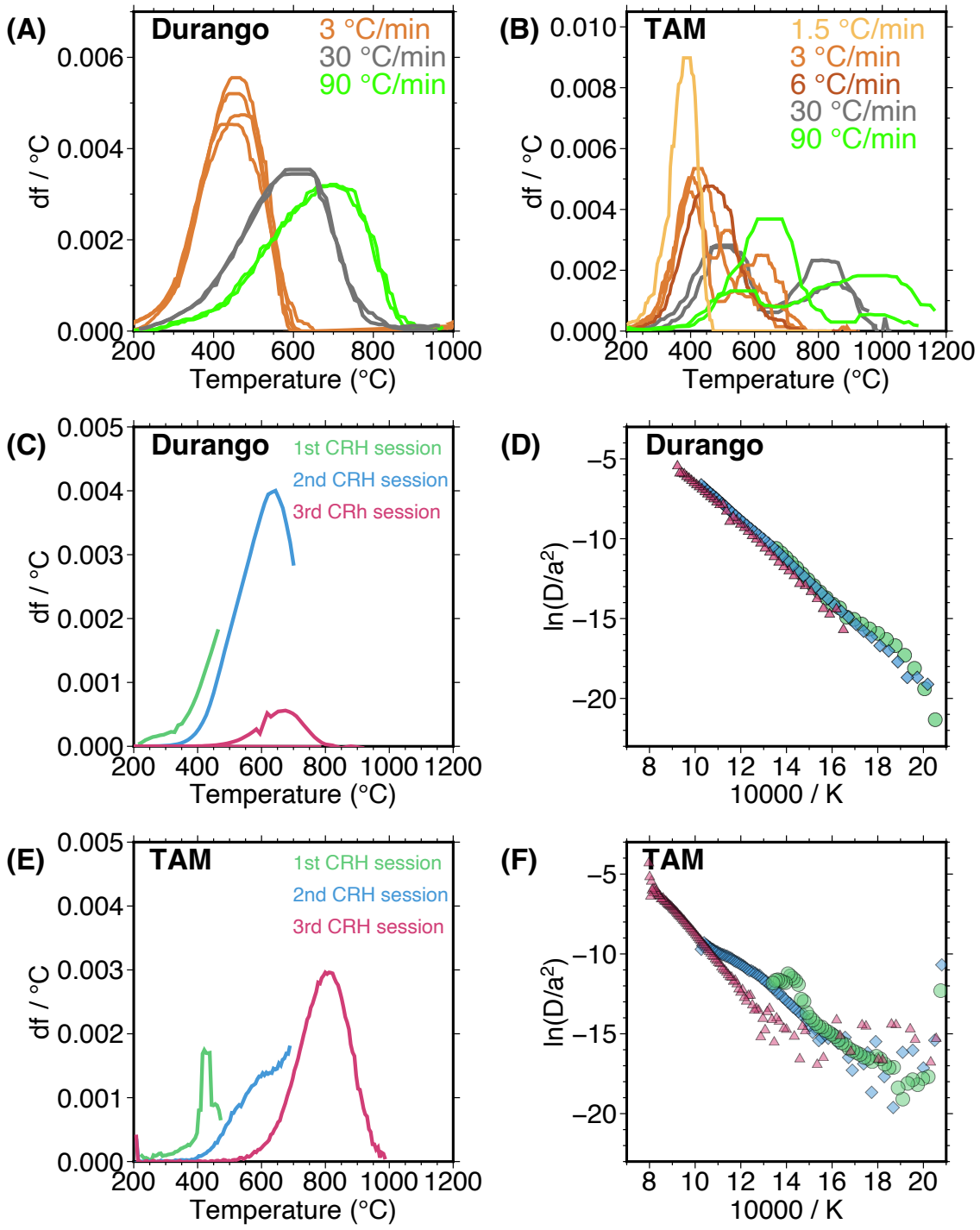
(A)
Durango
3 °C/min
30 °C/min
90 °C/min
df / °C
Temperature (°C)
(B)
TAM
1.5 °C/min
3 °C/min
6 °C/min
30 °C/min
90 °C/min
df / °C
Temperature (°C)
(C)
Durango
1st CRH session
2nd CRH session
3rd CRh session
df / °C
Temperature (°C)
(D)
Durango
ln(D/a²)
10000 / K
(E)
TAM
1st CRH session
2nd CRH session
3rd CRH session
df / °C
Temperature (°C)
(F)
TAM
ln(D/a²)
10000 / K

Fig. 2

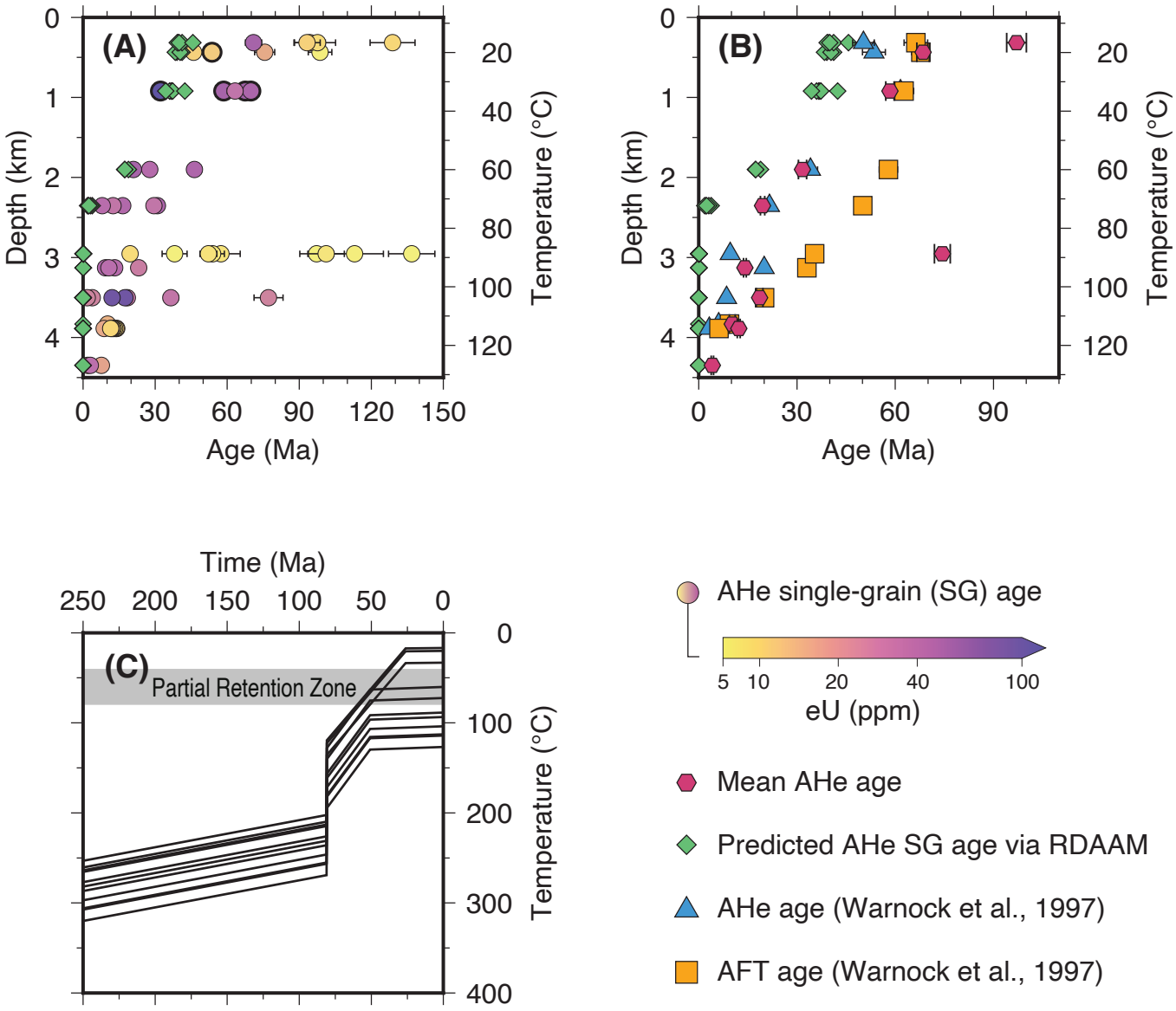
(A)
(B)
(C)
Depth (km)
Temperature (°C)
Age (Ma)
Time (Ma)
Partial Retention Zone
AHe single-grain (SG) age
eU (ppm)
Mean AHe age
Predicted AHe SG age via RDAAM
AHe age (Warnock et al., 1997)
AFT age (Warnock et al., 1997)

Fig. 3

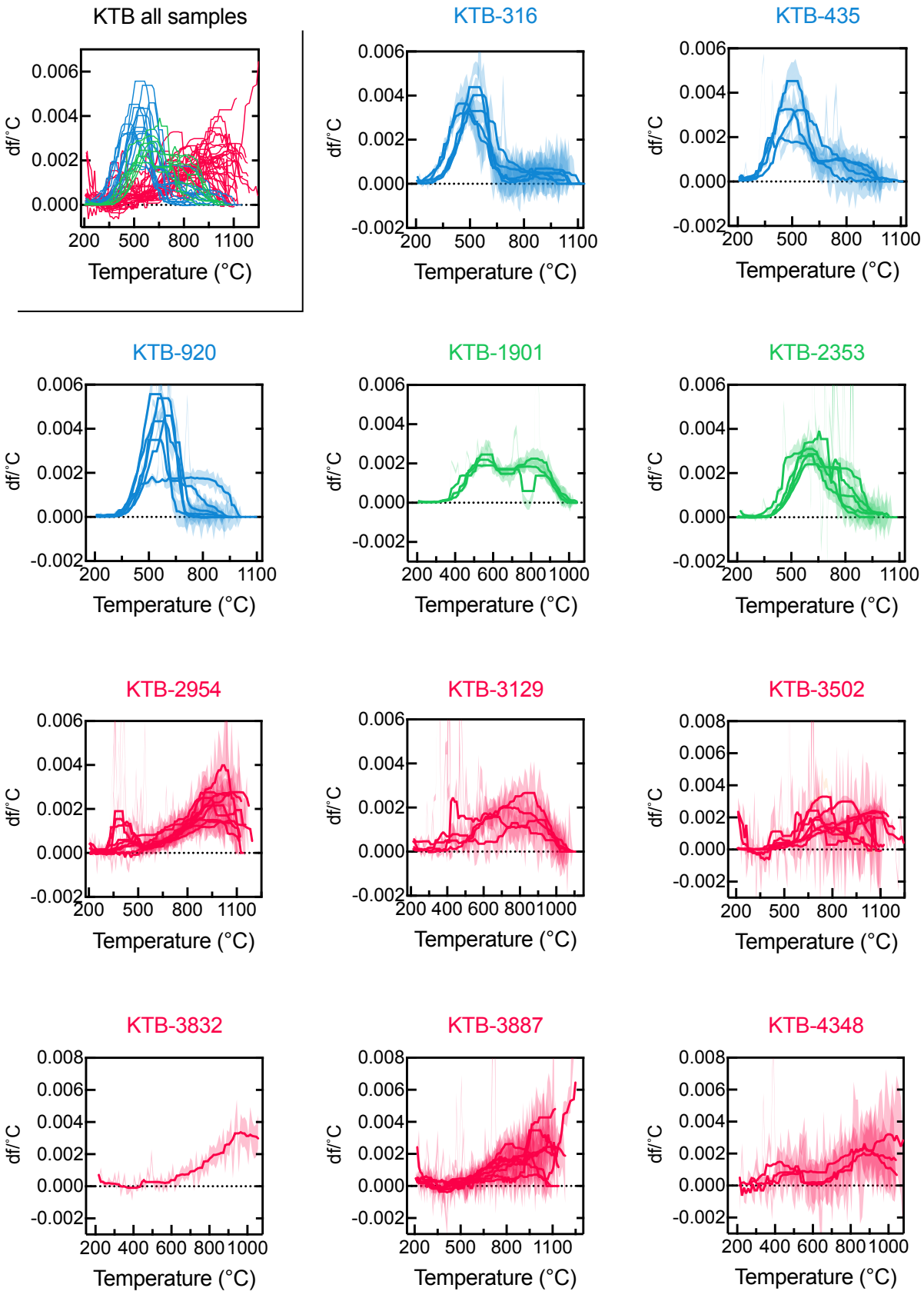
KTB all samples
KTB-316
KTB-435
KTB-920
KTB-1901
KTB-2353
KTB-2954
KTB-3129
KTB-3502
KTB-3832
KTB-3887
KTB-4348
df/°C
Temperature (°C)

Fig. 4

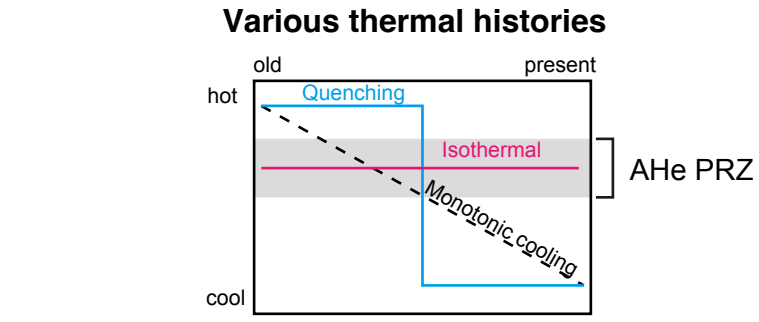
Various thermal histories
old
present
hot
cool
Quenching
Isothermal
Monotonic cooling
AHe PRZ

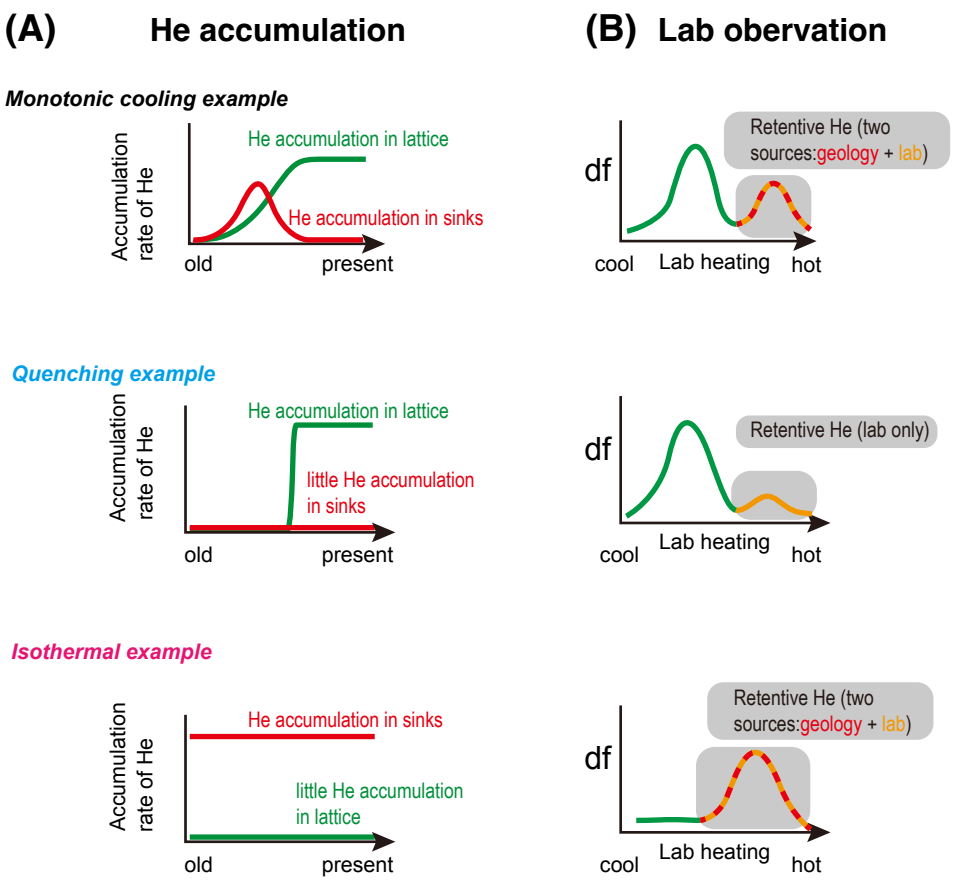
(A) He accumulation
(B) Lab obervation
Monotonic cooling example
Accumulation rate of He
He accumulation in lattice
He accumulation in sinks
old
present
df
Retentive He (two sources:geology + lab)
cool
Lab heating
hot
Quenching example
Accumulation rate of He
He accumulation in lattice
little He accumulation in sinks
old
present
df
Retentive He (lab only)
cool
Lab heating
hot
Isothermal example
Accumulation rate of He
He accumulation in sinks
little He accumulation in lattice
old
present
df
Retentive He (two sources:geology + lab)
cool
Lab heating
hot

Fig. 5

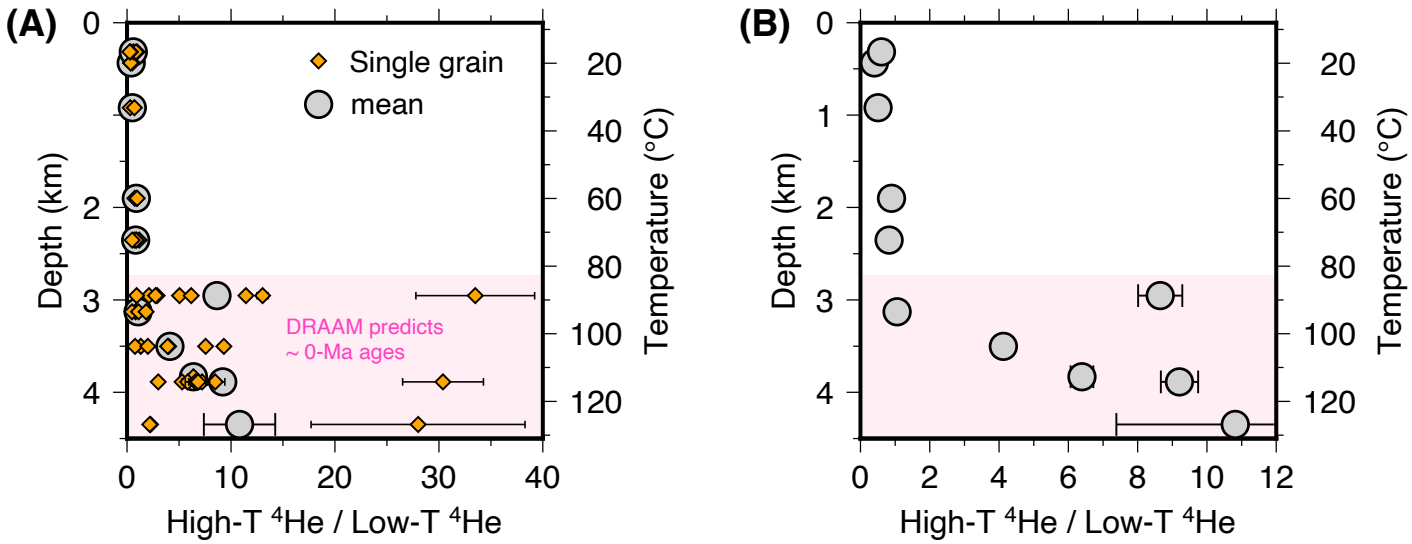
(A)
Single grain
mean
DRAAM predicts
~ 0-Ma ages
Depth (km)
Temperature (°C)
High-T 4He / Low-T 4He
(B)
Depth (km)
Temperature (°C)
High-T 4He / Low-T 4He

Fig. 6

Supplementary figure with caption

Figure A1. Individual df spectra for all KTB apatites. Black line: measured df. Orange lines are 11-point median-filtered df data. Uncertainty envelopes (2-sigma) are shown as transparent orange bands. Vertical grey bar denotes common temperatures at which the volume-diffusion governed gas-related peaks as observed from most Durango and TAM apatites.